10.1098/rsta.2001.0865

THE ROYAL SOCIETY

Computer simulation studies of the structure and dynamics of ions and non-polar solutes in water

By Jayendran C. Rasaiah[1] and R. M. Lynden-Bell[2]

[1]*Department of Chemistry, University of Maine, Orono, ME 04469, USA*
[2]*Atomistic Simulation Group, School of Mathematics and Physics, The Queen's University, Belfast BT7 INN, UK*

The mobility of simple ions such as alkali-metal and halide ions at room temperature shows two anomalies. Firstly, there are maxima in mobilities as a function of ion size for both positive and negative ions and, secondly, the maximum for negative ions occurs at a larger ionic radius than the maximum for positive ions. Theoretical treatments of this problem are reviewed and it is concluded that a molecular treatment of the system is needed to understand the results. Computer simulation using the simple point charge model (SPC/E) for water reproduced the observations and is used to discuss the application of theories. In particular, the nature of the first solvation shell is correlated with ion mobility. Simulation reveals a further anomaly, namely that if the charge is removed from a large ion, then it moves more slowly. This is interpreted as the result of formation of a solvent cage around the hydrophobic solute. The changes in local structure resulting from changes in charge and size also affect the solvation thermodynamics. Simulations show that the solvation entropy has a double maximum when viewed as a function of charge. The local minimum near zero charge is interpreted as being due to hydrophobic order, and the maxima as the result of structure breaking. This double maximum in the entropy of solvation is a signature of the hydrophobic cage effect. Comparisons are made between ion mobilities in liquid water at ambient and supercritical conditions.

Keywords: solvation; ion mobility; friction; hydrophobicity; simulation; supercritical

1. Introduction

Water is indispensable to life and is a solvent in many processes of chemical and biological interest. The properties of water are also very unusual (Franks 1973; Eisenberg & Kauzmann 1969). Of these, the best known is the maximum density at 4 °C, which influences its properties near melting. For example, ice floats on water, thus ensuring the survival of marine life in winter. The high dielectric constant of water at room temperature ($\varepsilon \approx 78$) favours the dissolution of ionic and polar species and renders hydrocarbons, inert gases and non-polar solutes relatively insoluble. This situation is completely reversed in the supercritical region that lies in the vicinity of the critical density of $0.32\,\mathrm{g\,cm^{-3}}$ and above the critical temperature of 640 K. The dielectric constant of water is low ($\varepsilon \approx 5$) in this region where it is a poor solvent for ionic

and polar solutes but a good solvent for non-polar species. The change in the dielectric constant of water with temperature has a profound effect on the properties of aqueous electrolyte solutions. For example, an aqueous solution of sodium chloride is a strong electrolyte at room temperature and a weak electrolyte at supercritical temperatures. Sodium chloride is thus completely dissociated into ions in aqueous solution at 298 K, but the little that dissolves in water above 640 K is strongly associated into pairs and possibly even clusters (Tester *et al*. 1998; Koneshan *et al*. 2001; Koneshan & Rasaiah 2000).

A detailed understanding of water requires a microscopic or molecular viewpoint (Stillinger 1980). There is a lot known about the spatial correlation between atoms in liquid water from X-ray and neutron diffraction studies, but surprisingly much more needs to be discovered, especially about changes in its structural and dynamical properties with temperature (Soper *et al*. 1997). Liquid water is neither a continuum dielectric nor is it a simple dipolar fluid, although its behaviour is often described in these terms as a first approximation. At a molecular level, the properties of water are ascribed to the asymmetric charge distribution in the molecule that favours a coordination number of four through hydrogen bonding, two of which are accepted and two donated. This arrangement leads to an open network structure in which the hydrogen-bonded neighbours are constantly switching allegiances in a promiscuous exchange of partners. It is the asymmetric charge distribution of the water molecule that differentiates between the solvation of positive and negative ions and breaks the symmetry of the simple dipolar description of this solvent (Koneshan *et al*. 1998*a*, *b*; Lynden-Bell & Rasaiah 1997).

2. Solvation dynamics and the mobility of ions in aqueous solution at infinite dilution

An ion dissolved in water polarizes the surrounding medium by changing the local orientation of the water molecules and by polarizing the electronic structure of individual molecules. The dynamics and the equilibrium electrostatics of this polarization have a direct influence on the transport coefficients and thermodynamics of solvation. In the continuum description of ions in solution, the free energy of hydrophilic solvation of an ion of radius R_i and charge q is given by the Born equation (see Robinson & Stokes 1959):

$$\Delta A_\mathrm{solv} = -\frac{q^2}{8\pi\varepsilon_0 R_\mathrm{i}}\left[1-\frac{1}{\varepsilon}\right], \tag{2.1}$$

where ε_0 is the permittivity of free space, and ε is the dielectric constant of the medium. Differentiation with respect to temperature leads to the entropy of solvation

$$\Delta S_\mathrm{solv} = \frac{q^2}{8\pi\varepsilon_0\varepsilon R_\mathrm{i}}\frac{\mathrm{d}\ln\varepsilon}{\mathrm{d}T}, \tag{2.2}$$

and the energy of solvation $\Delta U_\mathrm{solv} = \Delta A_\mathrm{solv} + T\Delta S_\mathrm{solv}$. For water at 298 K, $\varepsilon = 78.358$ and $\mathrm{d}\varepsilon/\mathrm{d}T = -0.3631\ \mathrm{K}^{-1}$, from which it follows that at room temperature (298 K), $\Delta A_\mathrm{solv} = -686q^2/R_\mathrm{i}\ \mathrm{kJ\,mol}^{-1}$ and $\Delta S_\mathrm{solv}/k = -4.9q^2/R_\mathrm{i}$ when the ion radius R_i is in angstroms. Thus, continuum theory predicts a parabolic dependence of the free energy, entropy and energy of solvation on the charge q. The thermodynamics

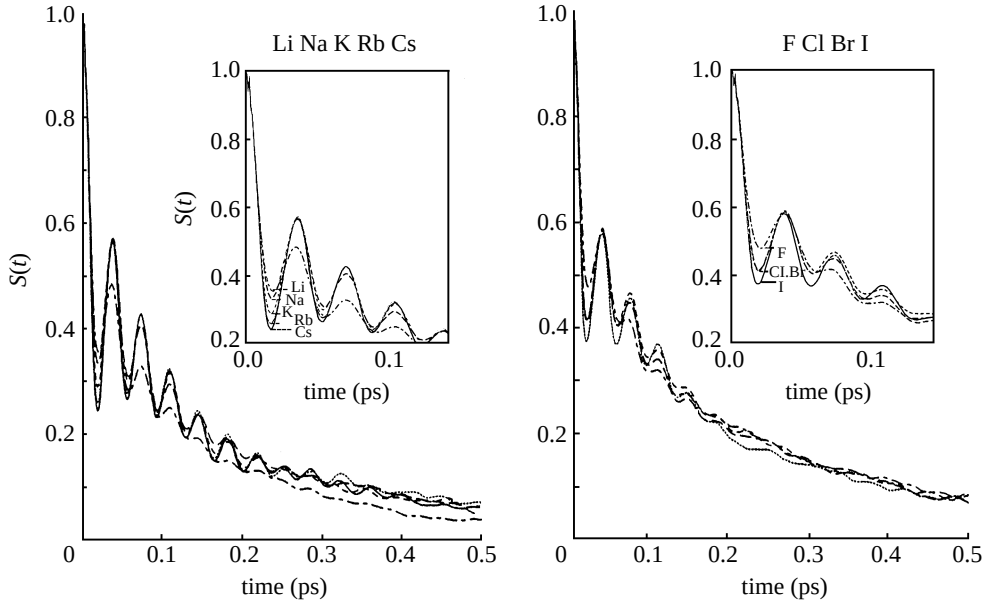

Figure 1. Solvation dynamics response function $S(t)$ of cations and anions at 298 K determined by molecular dynamics simulation of ions in SPC/E water (from Koneshan *et al.* 1998*a*, *b*).

of solvation of positive and negative ions of the same size are the same in this theory. This is contradicted by experimental data, and many attempts have been made to reconcile this discrepancy by adjusting the sizes of the positive and negative ions.

The entropy of solvation of non-polar solutes, like argon, at room temperature is negative. This has been discussed extensively starting with the early studies of Eley (1939*a*, *b*) and also Frank & Evans (1945) on the solubility of non-polar gases in water. The negative entropies of solvation of a non-polar solute were ascribed to the formation of ice-like patches in solution in the vicinity of the solute. More recently, computer simulations of simple non-polar solutes in water at room temperature reveal the presence of a hydrogen-bonded cage around a non-polar solute in water at ambient temperatures. Since the energy of solvation of a non-polar solute is small, the negative solvation entropy dominates the free energy ($\Delta A_{\mathrm{solv}} = \Delta U_{\mathrm{solv}} - T\Delta S_{\mathrm{solv}} \approx -T\Delta S_{\mathrm{solv}}$) rendering the solvation of a non-polar solute unfavourable in water at room temperature. This situation is described as hydrophobic solvation. The solvation free energy of polar and ionic solutes is, by contrast, dominated by the favourable enthalpy of solvation.

The solvation of an ion or polar solute is further characterized by its dynamics. Experimentally, the dynamics is inferred from time-delayed fluorescence shift (TDFS), spectroscopy in which the response of the solvent to the instantaneous polarization or charging of a fluorescing probe is followed with time (Jiminez *et al.* 1996; Rosenthal *et al.* 1994; Walker *et al.* 1992; Hornig *et al.* 1995; Maroncelli *et al.* 1989). Computer simulations also provide another route to solvation dynamics (Maroncelli & Fleming 1990; Vijaykumar & Tembe 1991; Perera & Berkowitz 1992; Neria & Nitzan 1992; Re & Laria 1997; Ladanyi & Maroncelli 1998; Koneshan *et al.* 1998*a*, *b*). In this method, an uncharged solute is equilibrated in a computer model

of a solvent like water, and the ion solvent electrostatic energy $U_{\rm solv}(t)$ is followed as a function of time, immediately after switching on a charge $\pm q$ on the solute. The same technique can be used to follow the solvent dynamics around a newly created dipolar solute. The function $S(t)$, which describes solvation dynamics, is defined by

$$S(t) = \frac{\langle U_{\rm solv}(t)\rangle - \langle U_{\rm solv}(\infty)\rangle}{\langle U_{\rm solv}(0)\rangle - \langle U_{\rm solv}(\infty)\rangle}, \tag{2.3}$$

where $\langle\cdot\rangle$ denotes an ensemble average. Figure 1 shows plots of $S(t)$ for various ions as a function of time determined at room temperature in computer simulations of the ions in water using the simple point charge model (SPC/E) for water carried out by Koneshan *et al.* (1998*a*, *b*), described further in § 3.

The response at room temperature consists of a rapid drop on a time-scale of *ca.* 25 fs followed by slow, oscillatory long-term relaxation over 1–5 ps. The initial phase in the solvent response $S(t)$ is attributed to fast librational motion of the solvent molecules accompanied by small amplitude oscillations. This is followed by translational and diffusive motions at longer times that account for the slower relaxation on a picosecond time-scale. The short-time solvation dynamics is different for positive and negative ions and depends on their size. The oscillations reflect the rotational and librational motion of the solvent molecules in readjusting to instantaneous charging of an ion. The long-time solvent response is a solvent property at a given temperature and is independent of the properties of the solute. This portion when fitted to an exponentially decaying function of time yields a characteristic relaxation time of *ca.* 0.5 ps at 298 K. The theory of the solvation dynamics of ions and polar solutes has been a very active field, developed independently by several workers (Wolynes 1987; Calef & Wolynes 1983; Nichols & Calef 1988; Rips *et al.* 1988*a*, *b*; Rips 1994; Bagchi & Chandra 1989; Bagchi 1989; Raineri *et al.* 1991, 1994, 1996; Raineri & Friedman 1994; Friedman *et al.* 1995; Maroncelli *et al.* 1993).

An important transport property that is modulated by the response of the solvent to a moving charge is the mobility $u_{\rm i}$ of an ion in aqueous solution (Robinson & Stokes 1959). This is just the drift velocity $\langle v_{\rm i}\rangle$ per unit electric field E, with $u_{\rm i} = \langle v_{\rm i}\rangle/E$ at low fields, when the response of the ion to the field is linear. In this region, the mobility of an ion is also related to the diffusion coefficient $D_{\rm i}$ in the absence of a field through the Stokes–Einstein relation:

$$u_{\rm i} = \frac{q_{\rm i} D_{\rm i}}{kT}. \tag{2.4}$$

Here k is Boltzmann's constant and T is the temperature in kelvin. The diffusion coefficient of an ion or uncharged solute is calculated from the asymptotic slope of the mean square displacement,

$$D_{\rm i} = \tfrac{1}{6}\lim_{t\to\infty}\frac{{\rm d}|(\boldsymbol{r}_{\rm i}(t) - \boldsymbol{r}_{\rm i}(0))|^2}{{\rm d}t}, \tag{2.5}$$

or from the integral of the velocity autocorrelation function:

$$D_{\rm i} = \frac{1}{3}\int_0^\infty \langle \boldsymbol{v}_{\rm i}(t)\cdot\boldsymbol{v}_{\rm i}(0)\rangle\,{\rm d}t. \tag{2.6}$$

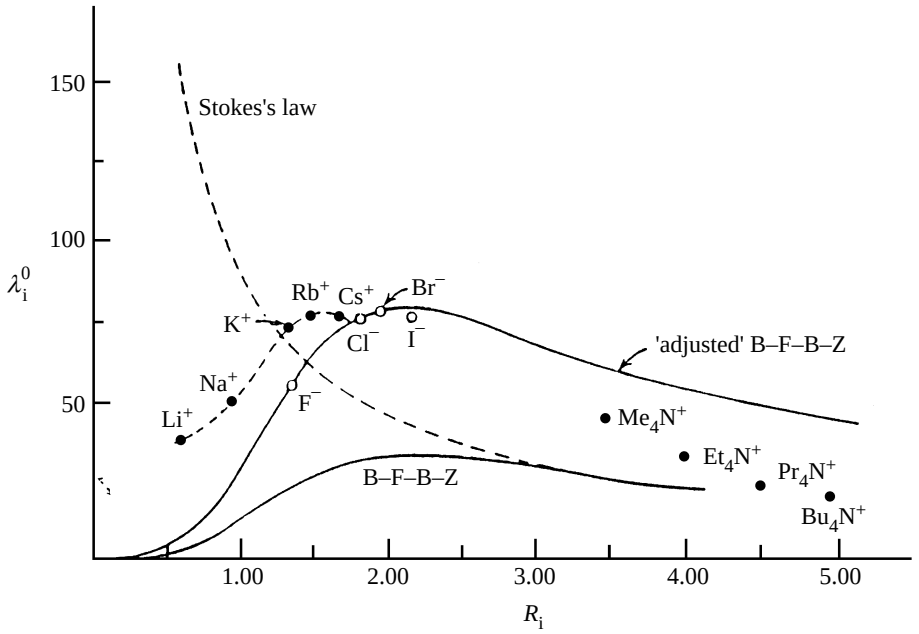

Figure 2. Ion conductivity at 298 K as a function of the crystallographic radius R_i (from Frank 1966).

Experimental results of ion mobility u_i are reported as the molar ionic conductance,

$$\lambda_i = FN_A u_i, \tag{2.7}$$

where N_A is Avogadro's number and the Faraday constant F is equal to 96 500 C.

At infinite dilution, interactions between the ions are absent and each ion moves independently of the others. This is Kohlrausch's law of independent migration. The conductance at infinite dilution is the sum of the conductivities of the ions:

$$\Lambda^0 = \nu_+\lambda_+^0 + \nu_-\lambda_-^0, \tag{2.8}$$

where ν_+ and ν_- are the stoichiometric coefficients that appear in the chemical equation for the dissociation of the electrolyte in solution.

The transport number of an ion at infinite dilution measures the fractional contribution of the ion to the total conductance, and can also be measured experimentally. Thus, the transport number of a positive ion is

$$t_+ = \frac{\lambda_+^0}{\Lambda^0}, \tag{2.9}$$

with an analogous definition for t_- with $t_+ + t_- = 1$. The mobilities of individual ions at infinite dilution follow from equations (2.8) and (2.9) and measurements of ion transport numbers and electrolyte conductivity.

Figure 2, from a paper by Frank (1966), shows the experimental λ_i^0 of positive and negative ions at room temperature plotted as a function of the crystallographic radius R_i of the ion.

A distinctive feature of this figure is that positive and negative ions lie on separate curves; each exhibiting its own maximum. It is strikingly clear that the smallest

and largest ions move more slowly than ions of intermediate size. The asymmetry in the mobilities of cations and anions immediately rules out a theoretical explanation based on a continuum description of water or representations of water as a molecule containing only an electric dipole or one with a perfect tetrahedral charge distribution of positive and negative charges. These models fail because their inherent symmetry cannot distinguish between positive and negative ions of the same size in solution. They do not contain a description of hydrogen bonds, which are essentially asymmetrical and play an important role in the properties of water.

The mobility of an ion at infinite dilution is determined by its interaction with the solvent and how this is coupled with interactions between solvent molecules. Both the energy and dynamics of these interactions are important. Theoretical discussions of diffusion and ion mobility are usually expressed in terms of the friction coefficient ζ, which is inversely proportional to the diffusion coefficient:

$$\zeta = kT/D_{\mathrm{i}}. \tag{2.10}$$

(*a*) *Continuum theory*

We begin with a discussion of continuum models, although it is not at all clear that they are applicable at the molecular level. The frictional resistance to the motion of an uncharged solute in a continuum solvent is entirely viscous, or hydrodynamic, and is assumed to follow Stokes's law:

$$\zeta_{\mathrm{V}} = K\eta R_{\mathrm{i}}. \tag{2.11}$$

Here ζ_{V} is the hydrodynamic friction, R_{i} is the radius of the solute, η is the solvent bulk viscosity, and the constant K is 6π or 4π, depending on whether stick or slip boundary conditions are used at the solute–solvent surface. Assuming stick boundary conditions, the diffusion coefficient of the uncharged solute

$$D_{i,0} = \frac{kT}{6\pi\eta R_{\mathrm{i}}}, \tag{2.12}$$

where the subscript '$i, 0$' implies zero charge on species i.

The electric field at the surface of large monovalent ions is relatively weak and their diffusion coefficients are also dominated by hydrodynamic friction. Examples are the large tetraalkyl ammonium ions $\mathrm{Pr_4N^+}$ and $\mathrm{Bu_4N^+}$. Hydrodynamic friction and the Stokes–Einstein relation leads to the following simple relation for the molar ionic conductivity by combining equations (2.4), (2.7) and (2.12):

$$\lambda_{\mathrm{i}}^0 = \frac{|z_{\mathrm{i}}|F^2}{6\pi\eta R_{\mathrm{i}}}. \tag{2.13}$$

Here z_{i} is the valence of the ion, the superscript '0' implies infinite dilution, and F is the Faraday constant. The Stokes law form of the hydrodynamic friction implies that the electrical conductivity increases as the ion size decreases. This behaviour is found only for large ions and does not apply to smaller ones, as illustrated in figure 2.

The molar conductivity of small ions actually decreases with the radius, and the conductivity of ions passes through a maximum as a function of size, signalling the failure of Stokes's law for small ions. One explanation for this breakdown is that the intense field in the vicinity of a small ion produces a tightly bound solvation

shell that moves along with the ion making it act like a large one. This is the classic 'solventberg' picture, which provides a plausible explanation for the low mobility of the Li^+ ion, since there is evidence that the water of hydration in the first shell is held firmly with a residence time of nearly 51 ps. Accordingly, the conductivity of Li^+ fits the Stokes law expression for an ion whose radius is the sum of the radii of the bare Li^+ and a water molecule. The solventberg picture fails, however, to account for the mobility of the Cl^- ion, which has a smaller residence time of *ca.* 13 ps and an effective solvated ion radius that is too large to account for its mobility on the basis of Stokes's law. The same model also fails to explain the mobilities of intermediate size ions like Na^+, Cs^+ and Br^- at room temperature. The Li^+ is accordingly a very special case because of its very small size and long-lived solvation shell.

An explanation of the mobilities of ions of varying size requires consideration of friction of a different kind, called dielectric friction, in addition to the hydrodynamic friction represented by Stokes's law. Ions moving in a polar solvent experience a frictional drag arising from the relaxation of the solvent polarization that does not instantaneously follow the moving ion. The dynamics of ion solvation and its relation to size should play a part in determining the magnitude of this term.

The subject of dielectric friction has been the focus of recent theoretical and computational studies and has been controversial (Koneshan *et al.* 1998*a*, *b*; Kumar & Maroncelli 2000). The first continuum description of dielectric friction was due to Born (1920), and it was followed by increasingly more sophisticated treatments by Fuoss (1959), Boyd (1961), Zwanzig (1963, 1970), Hubbard and co-workers (Hubbard 1978; Hubbard & Onsager 1977; Hubbard & Kayser 1981, 1982) and Adelman and co-workers (Chen & Adelman 1980; Nguyen & Adelman 1984). In Zwanzig's theory, which contains the essentials, the dielectric friction coefficient

$$\zeta_{\mathrm{D}} = B\frac{q^2(\varepsilon - \varepsilon_\infty)}{R_{\mathrm{i}}^3\varepsilon(1+2\varepsilon)}\tau_{\mathrm{D}}, \tag{2.14}$$

where $B = \frac{3}{4}$, τ_{D} is the Debye relaxation time, ε and ε_∞ are the static and high-frequency dielectric constants of the solvent, respectively, and q is the charge on the ion. Dielectric friction calculated from this theory is symmetrical in the charge, since it varies as the square of q and it is the same for positive and negative ions of the same size R_{i}. The variation with ion size is rapid, since ζ_{D} is proportional to R_{i}^{-3}.

The total friction is assumed to be the sum of the two contributions

$$\zeta = \zeta_{\mathrm{V}} + \zeta_{\mathrm{D}}, \tag{2.15}$$

where the first term is the hydrodynamic friction given by Stokes's law, and the second is the dielectric friction represented in Zwanzig's theory by equation (2.14). The solvent in this continuum theory is characterized by its viscosity η, the static and high-frequency dielectric constants ε and ε_∞, respectively, and a single relaxation time τ_{D}. Since ζ_{V} is proportional to R_{i} and ζ_{D} is proportional to R_{i}^{-3}, it follows that

$$\zeta = C_1R_{\mathrm{i}} + C_2R_{\mathrm{i}}^{-3} = \frac{C_1R_{\mathrm{i}}^4 + C_2}{R_{\mathrm{i}}^3}, \tag{2.16}$$

where C_1 and C_2 are constants determined by the properties of the solvent. Combining this with the expression for the diffusion coefficient in terms of the friction in

equation (2.10) we have

$$D_{\mathrm{i}} = \frac{kTR_{\mathrm{i}}^3}{C_2 + C_1 R_{\mathrm{i}}^4}, \tag{2.17}$$

which has a maximum at $R_{\mathrm{i}}^{\mathrm{m}} = (3C)^{1/4}$, in which $C = C_2/C_1$ is related to the solvent properties through η, ε_0, ε_∞ and τ_{D} and the charge q on the ion. The mobility of the ion is easily determined from this expression and the Stokes–Einstein relation (equation (2.4)). It leads to the following simple relation between the conductivity of an ion and its radius:

$$\lambda_{\mathrm{i}}^0 = \frac{AR_{\mathrm{i}}^3}{C + R_{\mathrm{i}}^4}, \tag{2.18}$$

where

$$A = \frac{|z_{\mathrm{i}}|F^2}{6\pi\eta}.$$

The above expression for the ionic conductivity was first derived by Frank (1966), who pointed out that it leads to a maximum in λ_{i}^0 as a function of ion size in qualitative agreement with experiment. This maximum is at $R_{\mathrm{i}}^{\mathrm{m}} = (3C)^{1/4}$, when

$$\lambda_{\mathrm{i}}^{0,\max} = A(3^{3/4}/4)C^{-1/4} \quad \text{and} \quad C = \frac{2}{3}\frac{\pi}{6}\left(\frac{\tau}{\eta}\right)\left(\frac{q^2}{\varepsilon_0}\right)\frac{\varepsilon_0 - \varepsilon_\infty}{\varepsilon_0},$$

assuming stick boundary conditions. Frank's plot of λ_{i}^0 versus R_{i} is reproduced in figure 2, in which the curve labelled B–F–B–Z stands for the Born–Fuoss–Boyd–Zwanzig theory represented by equation (2.18). The agreement between theory and experiment at room temperature is only qualitative unless, as Frank proposed, the viscosity is treated as an adjustable parameter. Good agreement can be obtained with the molar conductivities of the negative ions.

Chen & Adelman (1980) extended the continuum model further to include the effects of local solvent structure and dynamics by using an effective hydrodynamic radius R_{V} defined by

$$\frac{1}{R_{\mathrm{V}}} = (1 - \Delta)\frac{1}{R_{\mathrm{is}}} + \Delta\frac{1}{R_{\mathrm{i}}} = \frac{1}{R_{\mathrm{i}}}\left[\Delta + (1 - \Delta)\frac{R_{\mathrm{i}}}{R_{\mathrm{is}}}\right] \tag{2.19}$$

and an effective dielectric radius R_{D} defined by

$$\frac{1}{R_{\mathrm{D}}^3} = \frac{R_{\mathrm{is}}}{R_{\mathrm{i}}^4} f(\Delta, R_{\mathrm{i}}/R_{\mathrm{is}}, \varepsilon_{\mathrm{loc}}). \tag{2.20}$$

Here R_{is} is approximately equal to the size of the first solvation shell of the ion. Within that shell is defined a local density ρ_{loc}, viscosity η_{eff}, dielectric constant $\varepsilon_{\mathrm{loc}}$, and the solvation function,

$$\Delta = \frac{\eta\rho_{\mathrm{loc}}}{\eta_{\mathrm{eff}}\rho}, \tag{2.21}$$

in which η and ρ are the viscosity and density of the bulk solvent, respectively. The solvation function Δ is determined by the extent of ion solvation and has a value lying between 0 and 1, corresponding to rigid solvation and no solvation, respectively. The function $f(\Delta, R_{\mathrm{i}}/R_{\mathrm{is}}, \varepsilon_{\mathrm{loc}})$ interpolates smoothly between fully solvated and unsolvated limits, so that the recalculated hydrodynamic and dielectric friction

also interpolate smoothly between these limits. Note that even if there is complete desolvation in the sense that $\Delta = 1$, the dielectric radius may still be close to R_{is} if there is dielectric saturation in the first shell. The effective hydrodynamic and dielectric radii of an ion are both larger than the bare radius of small ions if they are strongly solvated. This leads to the notion that the dielectric friction is relatively weak for both very small and very large ions. It is weak for large ions because of their size, and weak for small ions like Li^+ which are strongly solvated, because the moving entity is the large solvated species: this is the classic 'solventberg' picture. A recent analysis of the friction coefficients of ions by Koneshan *et al.* (1998*a*) at 298 K supports this view.

These ideas have led to the notion that ionic friction can also be treated hydrodynamically in a semi-continuum theory using effective local and bulk viscosities determined by solvent relaxation in different regions around the ion. This was clarified further by a suggestion of Wolynes (1980) and Hubbard & Wolynes (1985) that the friction coefficient can be written as

$$\frac{1}{\zeta} = \int_{R_{\mathrm{i}}}^{\infty} \frac{\mathrm{d}r}{4\pi r^2 \eta(r)}. \tag{2.22}$$

Here R_{i} is the bare ion radius and is the local viscosity equal to the bulk value η at $r = \infty$. Impey *et al.* (1983) modelled the distance-dependent viscosity as a step function, with

$$\eta(r) = \begin{cases} \eta_{\mathrm{s}} & R_{\mathrm{i}} < r < R_{\mathrm{is}}, \\ \eta & r > R_{\mathrm{is}}, \end{cases} \tag{2.23}$$

where R_{is} is the radius of the coordination shell within which the viscosity is η_{s}. Substitution in (2.22) leads to

$$\frac{1}{\zeta} = \frac{1}{4\pi R_{\mathrm{i}}} F\left(\frac{\eta}{\eta_{\mathrm{s}}}, \frac{R_{\mathrm{i}}}{R_{\mathrm{is}}}\right), \tag{2.24}$$

in which

$$F\left(\frac{\eta}{\eta_{\mathrm{s}}}, \frac{R_{\mathrm{i}}}{R_{\mathrm{c}}}\right) = \left\{\frac{\eta}{\eta_{\mathrm{s}}} + \left(1 - \frac{\eta}{\eta_{\mathrm{s}}}\right)\frac{R_{\mathrm{i}}}{R_{\mathrm{is}}}\right\}. \tag{2.25}$$

This is unity for an unsolvated ion when $R_1 = R_{\mathrm{is}}$ and $\eta_{\mathrm{s}} = \eta$. If we neglect electrostriction and identify η_{s} with η_{eff}, (2.24) is identical to the Chen–Adelman expression for viscous friction. Impey *et al.* (1983) applied this model to the friction of ions in aqueous solution at room temperature, and Balbuena *et al.* (1996, 1998) used a similar model to interpret the mobilities of ions at supercritical temperatures.

The dielectric friction calculated in the continuum theory is proportional to the square of the charge, and is the same for positive and negative ions of the same size and charge magnitude. As noted already, this is contradicted by the experimental data for ion mobility in aqueous solution at room temperature. The qualitative difference in mobilities of cations and anions at room temperature can be traced to the charge asymmetry of the water molecule (Koneshan *et al.* 1998*b*), which requires a more detailed molecular theory of ion mobility.

(*b*) *Molecular theory*

A molecular theory of friction can be derived by starting with the generalized Langevin equation applied to ionic motion in a molecular solvent (Kubo *et al.* 1991;

Balucani & Zoppi 1994). The fluctuation dissipation theorem leads to an expression for the friction coefficient as the integral of the autocorrelation function of the random force on the ion

$$\zeta = \frac{1}{3kT}\int_0^\infty \langle \boldsymbol{F}_{\rm i}(t)\cdot\boldsymbol{F}_{\rm i}(0)\rangle \,{\rm d}t. \tag{2.26}$$

Here T is the absolute temperature, k is Boltzmann's constant, and $F_{\rm i}(t)$ is the random force on ion i exerted by the solvent at time t. This expression is the starting point of molecular theories of ionic friction beginning with Wolynes and co-workers (Wolynes 1978; Colonomos & Wolynes 1979; Hubbard *et al*. 1979) and developed further by Bagchi and co-workers (Biswas *et al*. 1995; Biswas & Bagchi 1997*a*, *b*; Bagchi & Biswas 1998) and others. The first major assumption in the theory of Wolynes is to equate the random force on the moving ion to the total force on a fixed ion, which is equivalent to treating the ion as a heavy Brownian particle. The second assumption is to decompose this force into hard and soft parts and neglect the cross terms.

The potential of mean force on the ion is given by

$$w_{\rm i}(r) = -kT\ln g_{\rm iw}(r), \tag{2.27}$$

where $g_{\rm iw}(r)$ is the orientationally averaged ion–water distribution function. This has a maximum as a function of r, with the force to the left of the maximum identified as repulsive or 'hard' and to the right identified as attractive or 'soft'. Splitting the force in this way into soft and hard parts subdivides the friction coefficient into three contributions:

$$\zeta = \zeta^{\rm HH} + 2\zeta^{\rm SH} + \zeta^{\rm SS}. \tag{2.28}$$

The first term $\zeta^{\rm HH}$ is the hard–hard contribution due to binary collisions between the solute and the solvent. It is also identified with the viscous drag embodied in Stokes's law. The last term $\zeta^{\rm SS}$ is the soft–soft term determined by structural rearrangements of the solvent modulated by solvent dynamics. It is identified loosely with dielectric friction, but this classification is open to debate, since dielectric friction may also include contributions form the cross terms $\zeta^{\rm SH}$ and $\zeta^{\rm HS}$, which are equal to each other. Wolynes neglected the cross terms, arguing that the time-scales associated with the hard and soft parts were widely different, and, in this approximation,

$$\zeta \approx \zeta^{\rm HH} + \zeta^{\rm SS}. \tag{2.29}$$

This theory reduces to the continuum limit when the solute–solvent interactions are weak and long ranged, and in the case of strong ion–solvent interactions to the solventberg limit in which the ion moves with its hydration shell. As a first approximation, Colonomos & Wolynes (1979) related $\zeta^{\rm SS}$ to the static mean square fluctuation $\langle F_{\rm S}^2\rangle$ of the soft force and its time dependence $\langle\tau_{\rm F}\rangle$ and found that

$$\zeta^{\rm SS} \approx \frac{1}{3kT}\langle F_{\rm S}^2\rangle\tau_{\rm F}. \tag{2.30}$$

The molecular theory was further extended and developed for ions in a simple dipolar fluid by Bagchi and co-workers (Biswas *et al*. 1995; Biswas & Bagchi 1997*a*, *b*; Bagchi & Biswas 1998), who retained the two main assumptions in the theory of Wolynes: namely the Brownian limit assumption and the neglect of the cross terms $\zeta^{\rm SH}$ and $\zeta^{\rm HS}$. Their calculation of the soft contribution, $\zeta^{\rm SS}$, to the friction takes account of

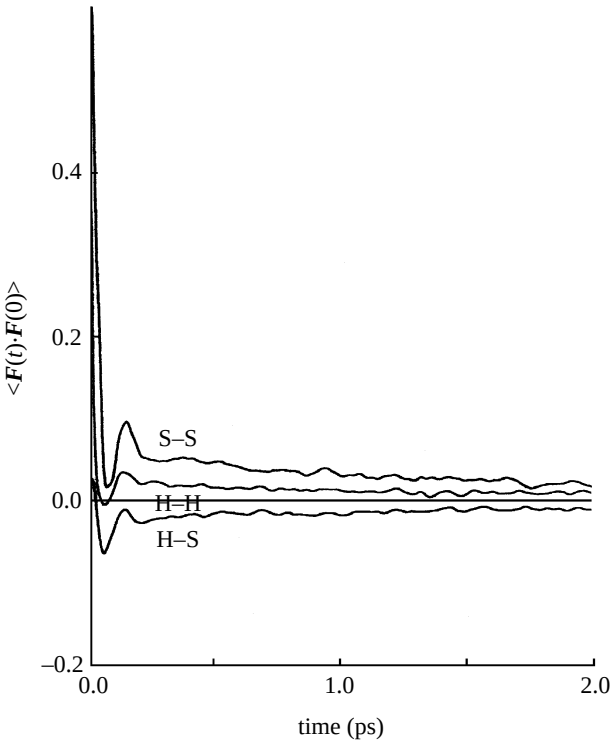

Figure 3. The components ζ^{HH} (hard–hard), ζ^{SS} (soft–soft) and ζ^{HS} (hard–soft) of the friction coefficients of the sodium ion in water at 298 K calculated from computer simulations of a fixed ion in SPC/E water (from Koneshan *et al.* 1998*a*, *b*).

the ultrafast solvent dynamics and the equilibrium solute–solvent correlations in the mean spherical approximation. The results of calculations of the mobility of cations in water, methyl alcohol and formamide are impressive, but the theory does not distinguish between cations and anions in water due to the simple dipolar symmetry of the model used for the solvent.

There is evidence from computer simulation studies of Wilson *et al.* (1985) that the friction coefficient of Na^+ in water calculated in fixed ion simulations is 60% larger than that calculated from the Stokes–Einstein relation and the diffusion coefficients determined with the velocity autocorrelation function of the moving ion. Also, molecular dynamics studies of Na^+ and Cl^- ions in water by Berkowitz & Wan (1987) and Tembe and co-workers (Sirdhar *et al.* 1993; Sivaprasad *et al.* 1994) have shown that the cross terms cannot be neglected, and this is confirmed in the more recent simulations of Koneshan *et al.* (1998*a*) shown in figure 3.

A recent molecular theory of ionic friction proposed by Chong & Hirata (1998, 1999*a*), using an interaction site model for the solvent and solute, considers a different separation of the random force autocorrelation function than the one used by Wolynes and others in which the cross terms are not neglected.

To summarize, the characteristic properties of the mobility or diffusion coefficients of ions and uncharged solutes that need explanation are

(i) the distinct curves for positive and negative ions;

(ii) the dependence on ion size with a characteristic maximum for each charge type;

(iii) the dependence on solvent structure and dynamics as determined by the equilibrium correlation functions and solvation dynamics; and

(iv) the dependence on charge, i.e. the difference in behaviour between the diffusion coefficients of charged and uncharged species of the same size.

Associated with this explanation is the identification of a minimal model for water that explains the differences between positive and negative ions at room temperature.

In what follows we discuss molecular dynamics simulations of ions in aqueous solution at infinite dilution. We identify a minimal model that accounts for the diffusion coefficients of charged and uncharged species dissolved in water at infinite dilution and the asymmetry in the free energy and entropy of solvation as a function of charge sign. The minimal model must of course incorporate the charge asymmetry of the actual water molecule. Fortunately, such models already exist; it is their ability to explain these phenomena that was not apparent until recently. The SPC/E model for water described in the next section satisfies these minimal requirements. Recently, Chong & Hirata (1999*b*) have used the same model in their theory to predict the mobilities of simple cations and anions in aqueous solution at room temperature. It is the first molecular theory to explain the differences in the mobilities of cations and anions of the same size in aqueous solution.

3. Computer simulation studies of the dynamics of ions in water at infinite dilution

Many convenient and useful potential energy functions for the interactions between two water molecules are available, such as three-, four- and five-site TIPS functions. The advantage of the SPC/E model with corrections for polarization discussed in this section lies not only in its accuracy and convenience, but in the simple extension of the same model to describe ion–water interactions with parameters fitted consistently to an experimental property. A consistent set of potential parameters for the simple cations and anions in water is of special importance in comparing differences in structural and dynamical properties of a family of ions that differ primarily in their sizes.

In the SPC/E model, a water molecule is treated as a collection of point charges distributed over the atomic sites with Lennard–Jones interactions between the oxygen atoms (Berendsen *et al.* 1987). The OH bond distances are fixed at 1.0 Å, and the bond angle between the two OH bonds of the water molecule is held at the tetrahedral angle of $109^\circ\,47'$. The intermolecular interaction between two water molecules has the form

$$u_{\mathrm{water}} = 4\varepsilon_{\mathrm{oo}}\left[\left(\frac{\sigma_{\mathrm{oo}}}{r_{\mathrm{oo}}}\right)^{12} - \left(\frac{\sigma_{\mathrm{oo}}}{r_{\mathrm{oo}}}\right)^{6}\right] + \frac{1}{4\pi\varepsilon_0}\sum_{i=1}^{3}\sum_{j=1}^{3}\frac{q_i q_j}{r_{ij}}. \tag{3.1}$$

The first term in this equation is the Lennard–Jones potential between the oxygen sites of distinct water molecules and the second is the electrostatic term in which q_{i} is the charge on site i, r_{ij} is the distance between sites i and j on two different water molecules, and ε_0 is the permittivity of free space. The parameters for this potential were determined by Berendsen *et al.* (1987) and are given in table 1. The

Table 1. *Halide–water, alkali-metal cation–water and water–water potential parameters (SPC/E model)*

(In the SPC/E model for water, the charges on H are at 1.000 Å from the Lennard–Jones centre at O. The negative charge is at the O site and the HOH angle is 109.47°. The Li^+ parameters are for the revised polarizability (RPOL) model.)

ion/water	σ_{io} (Å)	ε_{io} (kJ mol^{-1})	charge (q)
F^-	3.143	0.6998	−1
Cl^-	3.785	0.5216	−1
Br^-	3.854	0.5216	−1
I^-	4.168	0.5216	−1
Li^+	2.337	0.6700	+1
Na^+	2.876	0.5216	+1
K^+	3.250	0.5216	+1
Rb^+	3.348	0.5216	+1
Cs^+	3.526	0.5216	+1
Ca^{2+}	3.019	0.5216	+2
SPC/E	σ_{oo} (Å)	ε_{oo} (kJ mol^{-1})	charge (q)
$O(H_2O)$	3.169	0.6502	−0.8476
$H(H_2O)$			+0.4238

molecular dipole moment of SPC/E water is 2.35 D. This is larger than the dipole moment of a free water molecule (1.85 D) but smaller than the estimated dipole moment of water in ice, which is 2.6 D. The increased effective dipole moment of water in the liquid phase reflects the polarization of the molecule due to its neighbours. Guissani & Guillot (1993) and Guillot & Guissani (1993) determined the liquid–vapour coexistence curve for this model by computer simulation and found the critical parameters ($T_c = 640$ K, $\rho_c = 0.29$ g cm^{-3} and $P_c = 160$ bar). Except for the critical pressure, they are in good agreement with the critical parameters for real water ($T_c = 647$ K, $\rho_c = 0.322$ g cm^{-3} and $P_c = 221$ bar). The dielectric constant ε is 81 at 300 K and *ca.* 6 at 640 K, which agrees with the measured values of 78 and 5.3, respectively.

The SPC/E model has been used extensively over the past few years in computer simulation studies of the thermodynamic and transport properties of water (Berendsen *et al.* 1987) and ions in solution (Lynden-Bell & Rasaiah 1997; Koneshan *et al.* 1998*a*, *b*) and the results are in accord with the experimental results at room temperature. For example, a peak in the oxygen–hydrogen distribution functions $g_{oh}(r)$ at 1.8 Å, followed by a minimum at 3.3 Å, and a second peak at 4.5 Å, in the oxygen–oxygen distribution functions $g_{oo}(r)$, which is the signature of tetrahedral coordination, are observed in simulations of SPC/E water. The diffusion coefficient of SPC/E water at 25 °C also agrees well with the experimental result (Berendsen *et al.* 1987).

The ion–water potential used in our studies has a similar form:

$$u_{io} = 4\varepsilon_{io}\left[\left(\frac{\sigma_{io}}{r_{io}}\right)^{12} - \left(\frac{\sigma_{io}}{r_{io}}\right)^{6}\right] + \frac{1}{4\pi\varepsilon_0}\sum_{i=1}^{3}\sum_{j=1}^{3}\frac{q_i q_j}{r_{ij}}. \tag{3.2}$$

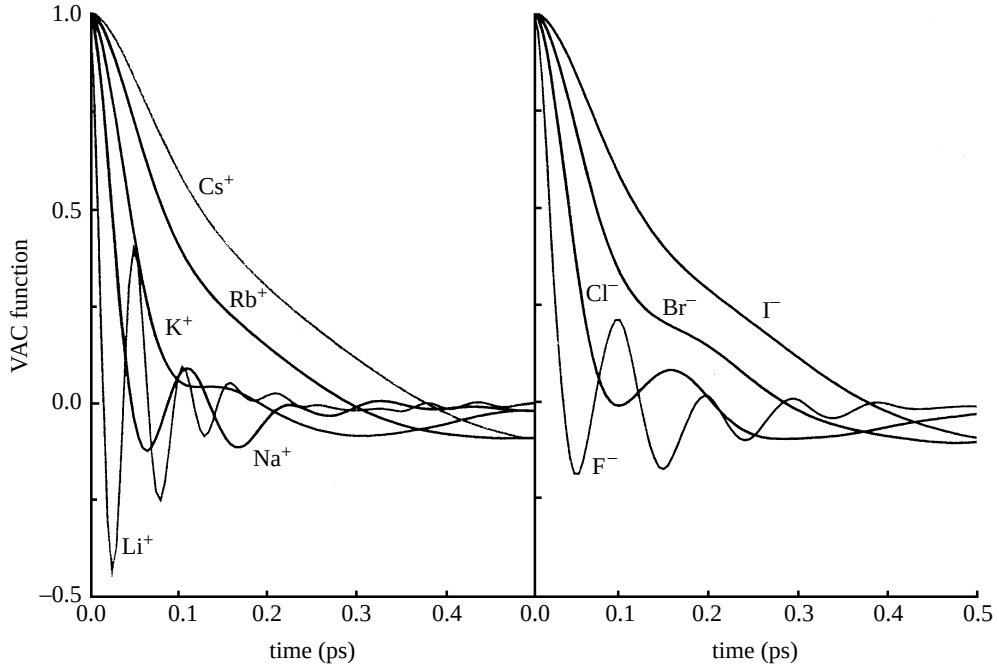

Figure 4. The normalized velocity autocorrelation functions of cations and anions in SPC/E water at 298 K calculated by computer simulation.

Here $\varepsilon_{\mathrm{io}}$ and σ_{io} are the Lennard–Jones parameters for the interaction between the ion and the oxygen atom 'o' of a water molecule, while the Coulomb term incorporates the electrostatic interactions between the charges on the oxygen and hydrogen sites of a water molecule and the charge on an ion. Dang and co-workers (Dang 1992*a*, *b*, 1995*a*, *b*; Dang & Garrett 1993; Dang & Kollmann 1995) fitted the parameters for this ion–water potential to the heats of solvation of small ion–water clusters containing from one to about 15 water molecules. The ions were the alkali-metal cations (Li^+, Na^+, K^+, Rb^+ and Cs^+), the halide anions (F^-, Cl^-, Br^- and I^-) and the divalent calcium (Ca^{2+}) and strontium (Sr^{2+}) ions. The parameters taken from Dang's papers are reproduced in table 1.

Molecular dynamics simulations of a single ion and 215 water molecules at room temperature (298 K) and a larger number (512) of water molecules at 683 K were carried out in the canonical ensemble with a time-step of 1 fs and a reaction field to take account of the long-range interactions (see Allen & Tildesley 1987; Frenkel & Smit 1996). The size of the cubical box was adjusted to the required density of water, which was 0.997 g cm^{-3} at 25 °C and 0.32, 0.2 and 0.997 g cm^{-3} in the supercritical region at 683 K. The simulations provide structural and dynamical information about a single ion and its interaction with the surrounding water molecules. The reader is referred to the original publications for further details. The diffusion coefficients were determined either from the mean square displacements or the velocity autocorrelation functions (Rasaiah *et al*. 2000; Noworyta *et al*. 2000) shown in figure 4 and found to be in good agreement with each other.

The most significant finding is that the diffusion coefficients and mobilities of the ions at 25 °C fall on two separate curves as a function of their ion size with

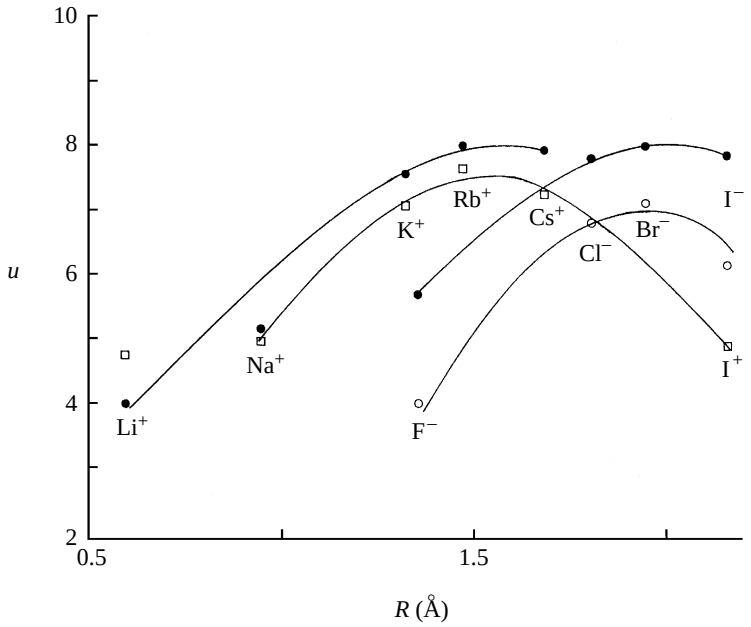

Figure 5. Ion mobility (units of 10^{-8} m^2 V^{-1} s^{-1}) as a function of the crystallographic radius R in angstroms calculated from computer simulations of anions (○) and cations (□) in SPC/E water. The experimental results are shown as filled circles (●) (from Koneshan *et al.* 1998*a*, *b*).

a maximum for each charge type. It is evident from figure 5 that a plot of the mobility, u_{i}, versus the Lennard–Jones parameter, σ_{io}, follows the same pattern as the experimental results.

Simply changing the charge on an I^- ion from negative to positive to generate an I^+ ion, keeping the Lennard–Jones ion–water parameters for I^- and I^+ unchanged, allows the range of cation sizes to be extended. The I^+ represents a purely fictitious large cation.

In an analogous way, turning off the charges on ions generates a family of uncharged solutes or 'drones', whose diffusion coefficients can be determined from the mean square displacement in the usual way. The diffusion coefficients of the ions and uncharged solutes are displayed in figure 6 as a function of the Lennard–Jones parameter σ_{io}.

Two important conclusions emerge from this study.

(a) With the possible exception of the smallest solute Li^0, Stokes's law is obeyed by neutral atomic sized solutes moving in water, even though the solvent molecules have a comparable size with the solute. This is seen in the plot of the friction coefficient as a function of solute size σ_{io} shown in figure 7. The viscosity of SPC/E water at 25 °C calculated from the slope of the Stokes law plot in figure 6 assuming slip boundary conditions is 1.73×10^{-3} kg m^{-1} s, which is within a factor of two of the experimental result (0.89×10^{-3} kg m^{-1} s) for pure water at 25 °C.

(b) Turning off the charge on the small ion Li^+ increases its diffusion coefficient, while the opposite is true for the large ions I^- and I^+. The behaviour of Li is

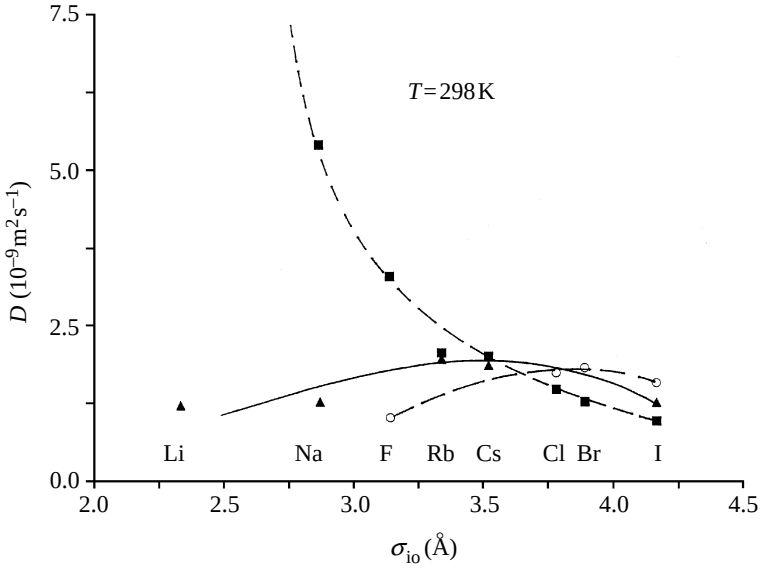

Figure 6. Diffusion coefficients (units of 10^{-9} m^2 s^{-1}) of cations (▲), anions (○) and uncharged solutes or 'drones' (■) at 298 K as a function of the size represented by the Lennard–Jones parameter σ_{io}. The curves are drawn as an aid to the eye (from Koneshan *et al.* 1998*a*, *b*).

easily understood in terms of the solventberg picture. The lithium ion loses its tightly bound solvation shell when stripped of its charge, reducing its size and making it able to move faster in solution, as predicted by Stokes's law. The behaviour of large solutes, e.g. I^-, after charge neutralization presents a puzzle that led to a detailed study of the structure and dynamics of the solvation ions and neutral species.

The ion–oxygen pair distribution function $g_{\mathrm{io}}(r)$ is related to the probability that the oxygen atom of a water molecule resides at a distance r from an ion. Figure 8 shows the ion–oxygen pair distribution functions for I^-, and the fictitious I^+ and I^0 determined by computer simulation. The uncharged I^0 has a prominent peak, and visual inspection of an equilibrated configuration of water in the first hydration shell reveals a cage around the solute held together by hydrogen bonds. This is hydrophobic solvation.

The charge asymmetry of the water molecule accounts for the difference in the solvation of positive and negative ions, particularly due to the orientation of water molecules in the first shell. The oxygen atom of a water molecule in the hydration shell of a cation lies closer to the ion than do the hydrogen atoms, while for anions one of the two hydrogen atoms of the water of hydration is closer than the oxygen. In the latter case the water hydrogen forms a hydrogen bond to the anion, and it is evident from figure 8 that this difference in the ion–water interaction allows the oxygen to approach I^- more closely than the fictitious I^+.

The coordination number N_{h} of the solute is obtained as a volume integral of solute (s) or ion (i)–oxygen pair distribution function $g_{\mathrm{io}}(r)$ from the relation

$$N_{\mathrm{h}} = \rho_{\mathrm{w}} \int_0^{R_{\mathrm{h}}} g_{\mathrm{io}}(r) 4\pi r^2 \, \mathrm{d}r. \tag{3.3}$$

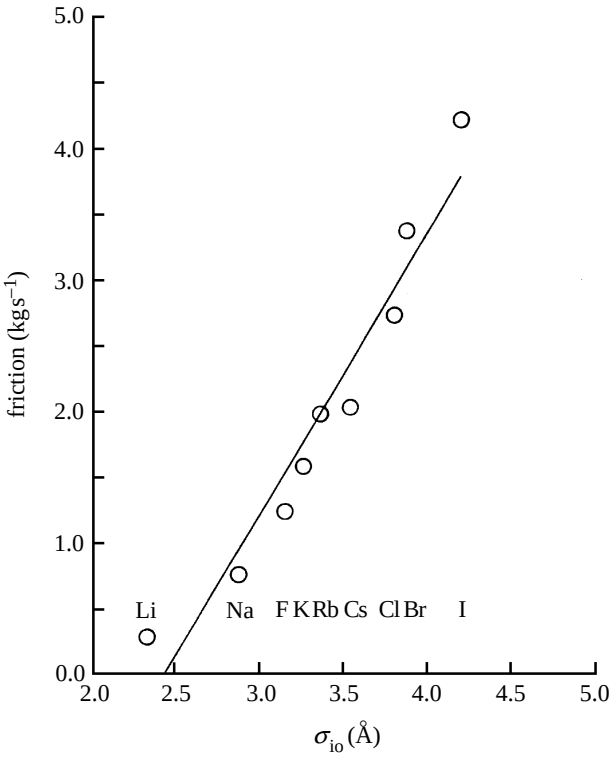

Figure 7. Friction coefficients (kg s^{-1}) versus size σ_{io} for uncharged solutes in SPC/E water at 298 K, showing that the Stokes law is obeyed reasonably well by uncharged solutes of atomic size with the possible exception of the smallest (Li^0). The solid line corresponds to Stokes's law (from Koneshan *et al.* 1998*a*, *b*).

Here R_h is the position of the first minimum in the pair distribution function, and ρ_w is the number density of the solvent. The coordination numbers in the primary solvation shells of I^-, I^+ and I^0 at 25 °C and a solvent density of 0.997 g cm^{-3} are *ca.* 8, 25 and 27, respectively. This means that the uncharged I^0 is more heavily hydrated than the ions I^- or I^+. The hydration numbers of ions and 'drones' are plotted as a function of size in figure 9, which shows that they increase with solute size.

The dynamics of the hydration shells are characterized by the residence time τ_{res} of water in the shells, defined as

$$\tau_{res} = \int_0^\infty R(t)\,dt, \tag{3.4}$$

where $R(t)$ is the residence time correlation function introduced by Impey *et al.* (1983) and defined by

$$R(t) = \frac{1}{N_h}\sum_{i=1}^{N_h}\langle\theta_i(t)\theta_i(0)\rangle, \tag{3.5}$$

in which $\theta(t)$ is the Heaviside step function that is 1 if the water molecule i is in the coordination shell of the ion at time t and zero otherwise. The residence time

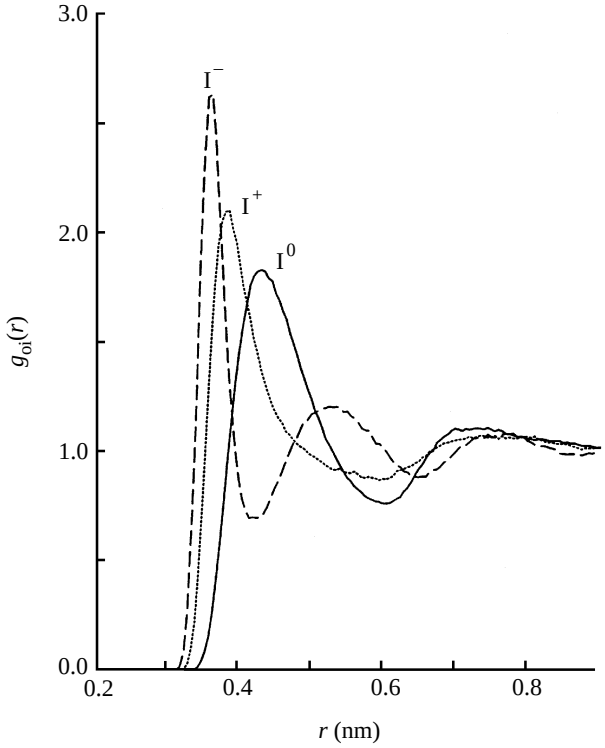

Figure 8. Ion–oxygen radial distribution functions for I^-, I^+ and I^0 in SPC/E water at 298 K (from Koneshan *et al*. 1998*a*, *b*).

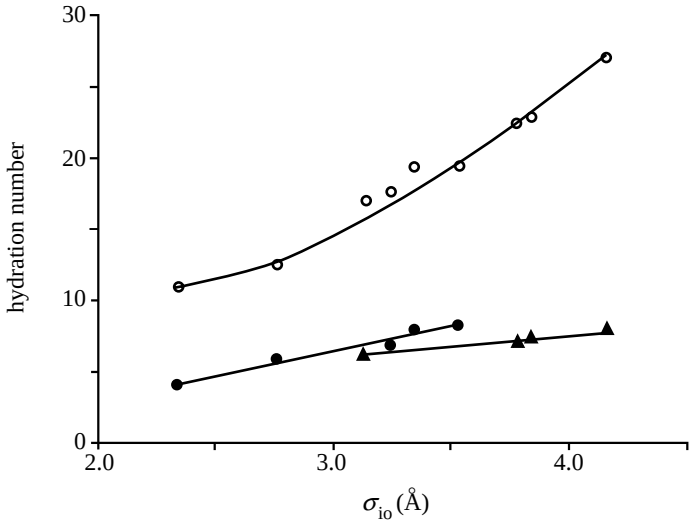

Figure 9. Hydration numbers of ions and uncharged species or 'drones' at 298 K in SPC/E water (○, uncharged solutes; ●, cations; and ▲, anions).

Table 2. *Average coordination numbers and residence times* (ps) *of water in the primary hydration shell of an ion and the corresponding discharged species in SPC/E water at* 25 °C

(The residence times in parentheses are calculated from the residence time correlation function, which does not allow for a 2 ps excursion time.)

ion	hydration number	residence time (ps)	
F^-	6	24	(24)
F	17	19	(16)
Cl^-	7	17	(13)
Cl	23	22	(18)
Br^-	8	13	(11)
Br	23	26	(20)
I^-	8	14	(9)
I	27	28	(24)
I^+	25	21	(19)
Li^+	4	54	(51)
Li	11	8	(4)
Na^+	6	22	(20)
Na	13	13	(9)
K^+	7	14	(9)
K	18	18	(14)
Rb^+	8	12	(10)
Rb	19	20	(17)
Cs^+	8	14	(10)
Cs	20	20	(16)
Ca^{2+}	8	700	(700)
Ca	16	14	(10)
H_2O (SPC/E)	4.4	5.6	

correlation functions of I^0, I^+ and I^- are shown in figure 10, and the hydration numbers and residence times of different ions and uncharged solutes at 298 K are displayed in table 2. All the ions and neutral solutes have residence times at this temperature that are larger than the residence time of water in its first coordination shell.

A plot of τ_{res} as a function of the size parameter σ_{io} (shown in figure 11) reveals a minimum for cations as the size increases, signalling a crossover from hydrophilic to hydrophobic solvation for positive ions. The residence times for anions decrease with their size, while those for uncharged molecules increase with size.

The order of the residence times for charged and uncharged iodine is

$$\tau_{\mathrm{res}}(I^0) > \tau_{\mathrm{res}}(I^+) > \tau_{\mathrm{res}}(I^-),$$

which is the reverse of the order of the diffusion coefficients:

$$D(I^0) < D(I^+) < D(I^-).$$

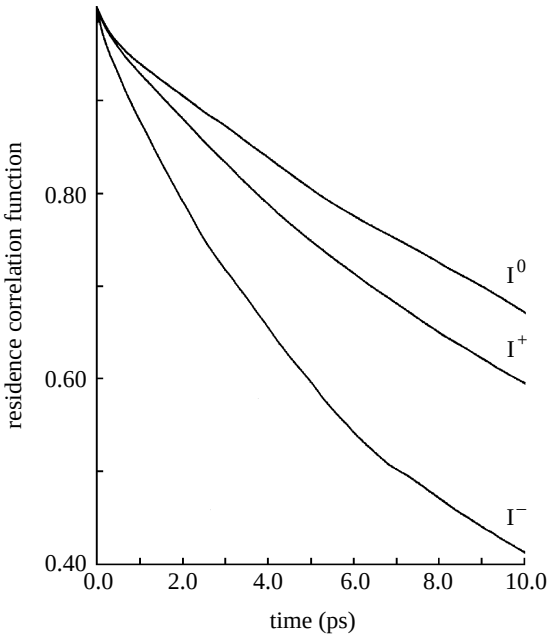

Figure 10. Residence time correlation functions for I^-, I^+ and I^0 in SPC/E water at 298 K.

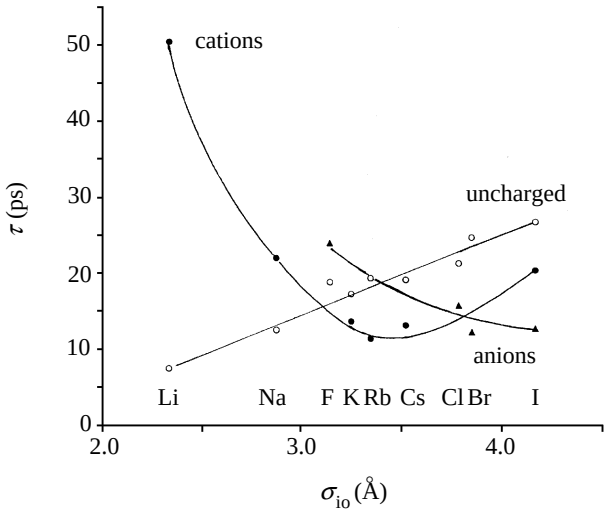

Figure 11. Residence times of cations, anions and uncharged species as a function of their size (from Koneshan *et al*. 1998*a*, *b*).

These trends suggest that hydrophilic electrostatic solvation of a small ion is radically different from the hydrophobic solvation of an uncharged solute enclosed in a cage of water molecules held together by hydrogen bonds. The cage around I^0 is partly broken when the solute is charged, enabling the ion to move faster and accounting qualitatively for the increase in diffusion coefficient of I^- over I^0. Comparison of the diffusion coefficients of I^+ and I^- and the corresponding residence times (25 ps for I^+

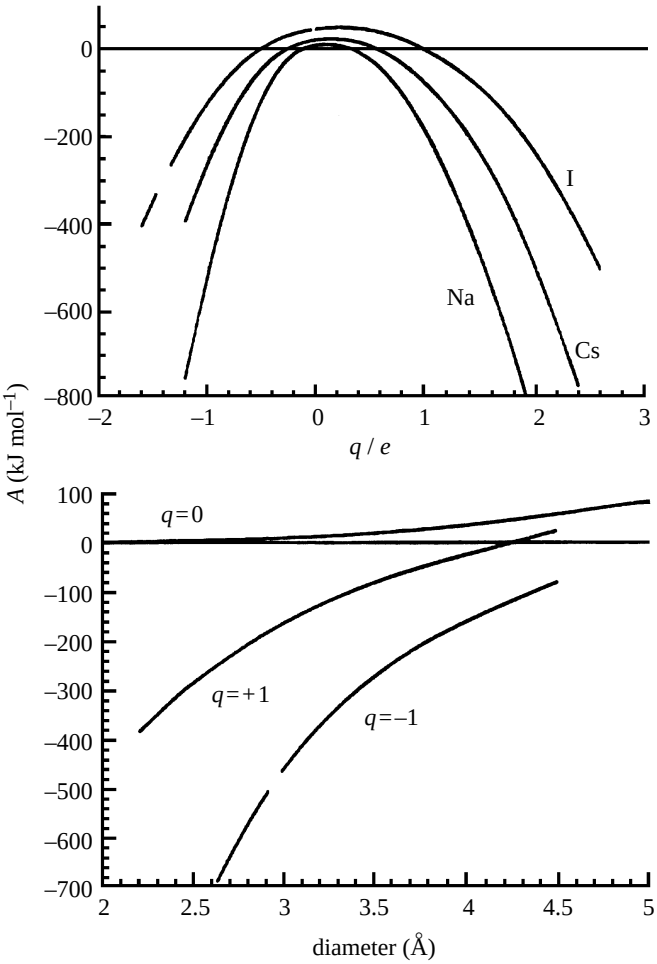

Figure 12. The variation of solvation free energy $A(q, \sigma)$ with charge q (a) and size σ (b). (a) The curves belong to sodium, caesium and iodine families with diameters of 2.876, 3.25 and 4.126 Å. (b) The figures belong to $q = 0$, $+1$ and -1 (from Lynden-Bell & Rasaiah 1997).

versus 8 ps for I^-) suggests that I^+ hydration is still largely hydrophobic, while the hydration of I^- has a greater degree of hydrophilic character to it. This is explained by the close proximity and orientation of water in the first shell of the anion I^-, in contrast to the water of hydration of I^+. It also suggests a possible correlation between the diffusion coefficients and the thermodynamics of hydration of ions of varying charge and sign discussed in the next section.

4. Computer simulation of the thermodynamics of ion solvation

The molecular nature of the solvent causes deviations from the simple Born model described in § 2. Computer simulation shows effects which can be associated with hydrophobicity and hydrophilicity. The predictions of the Born model are that the free energy, entropy and internal energy are simple parabolic functions of the charge and reciprocal functions of the ion radius. The change in solvation free energy

$A_{\mathrm{solv}}(q, \sigma)$ of a Lennard–Jones sphere as a function of the charge q and the size σ can be measured by a number of techniques, such as the extended dynamics used by Lynden-Bell & Rasaiah (1997). The internal energy changes can be measured directly, although the results tend to be somewhat noisy. The entropy of solvation is then found from the difference. Figure 12 shows the free energies of solvation plotted as a function of the charge (above) and size (below). The asymmetry between the positively charged ions and the negatively charged ions is clear in both parts. In the upper part the curves are steeper for negative values of the charge than for positive values, while the curves for constant charge shown below show that the free energy of solvation of positive ions is only *ca.* 50% of that of negative ions.

The reason for this can readily be found by examining the orientations of the water molecule in the first shell of the solute (Impey *et al.* 1983; Bergmann *et al.* 1999). The water around positively charged ions preferentially aligns with their dipole axis pointing in the radial direction, while negatively charged ions interact preferentially with one of the two protons of a water molecule, so that it is an OH bond rather than the dipole moment that is aligned along the radial direction.

This asymmetry between the solvation of positive and negative ions is due to the fact that negative ions act as strong hydrogen bond acceptors, while positive ions cannot act as hydrogen bond donors.

The variation of the entropy (in units of Boltzmann's constant k of solvation with charge demonstrates the importance of the entropy in hydrophobicity. Figure 13 shows the variation of the solvation entropy with charge (above) and size (below).

The striking aspect of these curves is the appearance of maxima. In particular there is a double maximum in the entropy versus charge which is quite different to the single maximum at zero charge predicted by the Born model and shows the special properties of water as a solvent. The entropy minima near $q = 0$ are signatures of the hydrophobic effect, which is associated with an abnormally high negative entropy of solvation. The water molecules in the first shell around a hydrophobic solute are arranged with their dipole moments tangential to the solute so that they can hydrogen bond to each other. As the magnitude of the solute charge is increased, these water molecules rotate, disrupting the water network and initially increasing the entropy. As the magnitude of the charge is increased further, the order induced by the electric field of the solute outweighs the disorder caused by disrupting the network, so that the entropy of solvation decreases. It is possible to use simulation to probe these observations in more detail. Bergmann *et al.* (1999) measured the two-body solute–water contributions to the solvation entropy and found that, although they are dominant at high charges, they do not give a hydrophobic minimum at low charges. This supports the idea that the hydrophobic effect is a consequence of the water–water network structure.

The entropy maxima, where there is most structure, are more pronounced for negative charges than for positive charges and shift to higher magnitudes of the charge when the solute size is increased. One might expect that the points of maximum structure breaking are places where the first shell is most disrupted. In fact this is not easy to demonstrate (Bergmann *et al.* 1999). One can, however, correlate the maximum entropy with the disappearance of the second shell in the solute oxygen radial distribution function. This is shown in the central traces of figure 14.

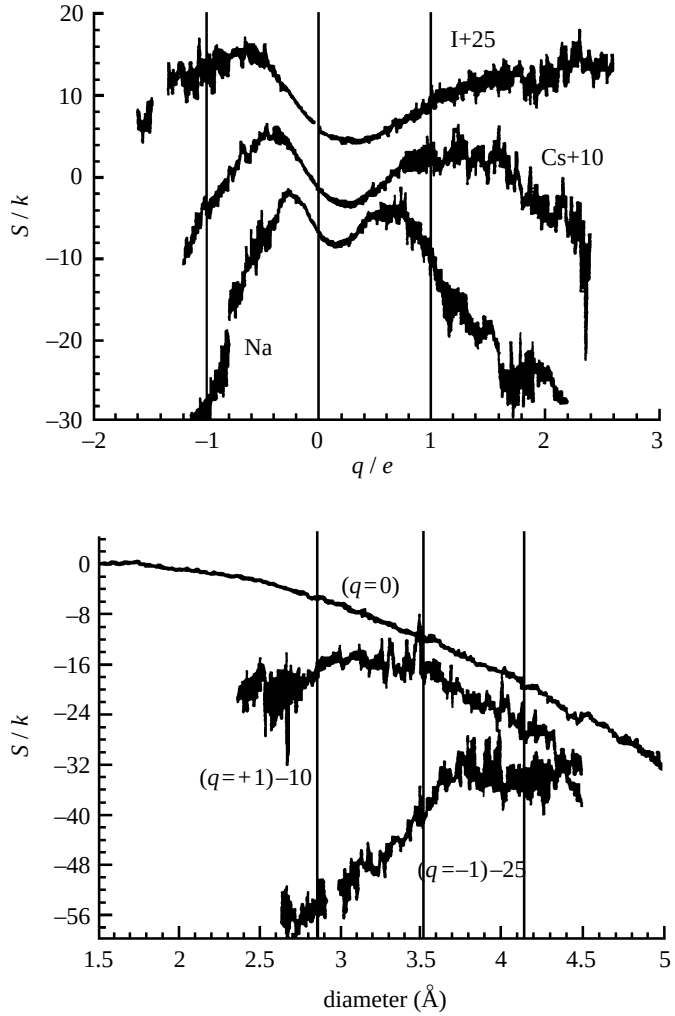

Figure 13. Variation of solvation entropy (in units of Boltzmann's constant k) with charge (a) and size (b). The curves are displaced by the amounts shown for clarity (from Lynden-Bell & Rasaiah 1997).

The upper curves in this figure show the distributions around charged ions, while the bottom curves show the distribution around hydrophobic solutes. The separation between the first and second shells changes from 3 Å to just over 2 Å for $q = +1$ to $q = -1$. This reflects the water structure around hydrophilic and hydrophobic solutes.

5. Supercritical water

We conclude this review with a brief account of our studies of ions and simple non-polar solutes dissolved in supercritical SPC/E water at a temperature of 683 K, which is nearly 40 K above the critical temperature of real water and the model SPC/E water. The critical density of water is nearly $0.32\,\mathrm{g\,cm^{-3}}$. Supercritical water is

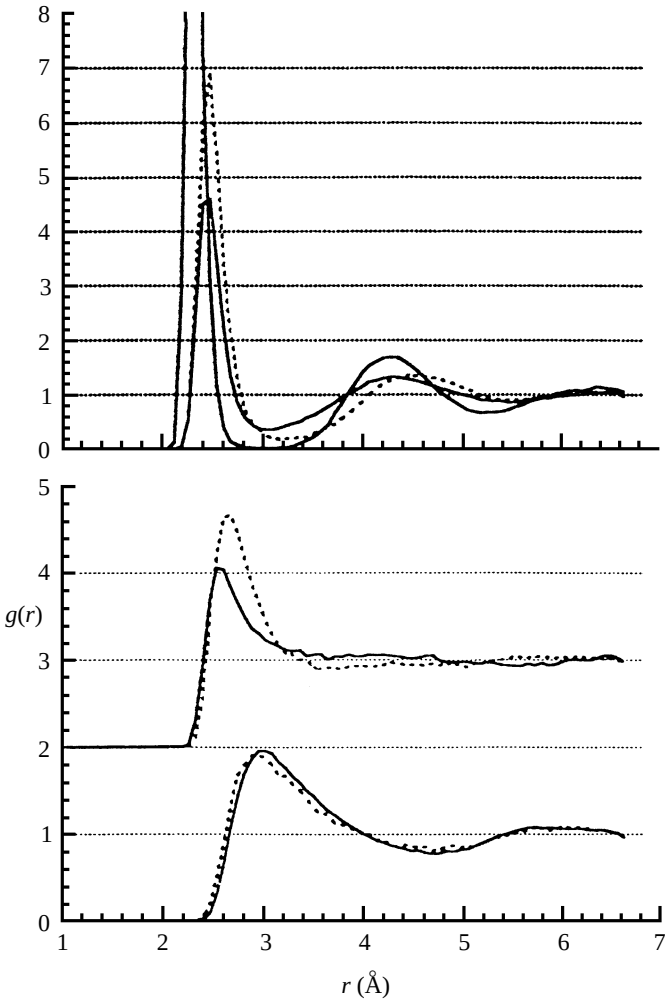

Figure 14. Solute–oxygen distribution functions for the sodium family. Top: examples with low entropy due to hydrophilic order ($q = -1$, $+1$ and -0.5, dotted line). The middle set of curves belong to values of the charge near the entropy maxima ($q = -0.3$, dashed line, $+0.5$), and the bottom set of curves correspond to regions of low entropy due to hydrophobic order ($q = 0$, $q = 0.2$, dashed line) (from Lynden-Bell & Rasaiah 1997).

characterized by large density fluctuations with voids continually forming and filling up, particularly at low density (Tucker 1999). Water is highly compressible in this region, and the density is easily fine tuned by changing the external pressure.

Recent computer simulation studies (Rasaiah *et al.* 2000; Noworyta *et al.* 2000) show that the hydration numbers of small ions (e.g. Li^+, Na^+) at 683 K and a solvent density of 0.35 g cm^{-3} are nearly the same as the corresponding values at 298 K and a solvent density of 0.997 g cm^{-3}. They are weakly dependent on the solvent density over the range 0.2–0.997 g cm^{-3} at high temperatures and become slightly smaller as the density decreases. In contrast to this, the residence times of water in the primary hydration shells of ions are lower by an order of magnitude at 683 K than

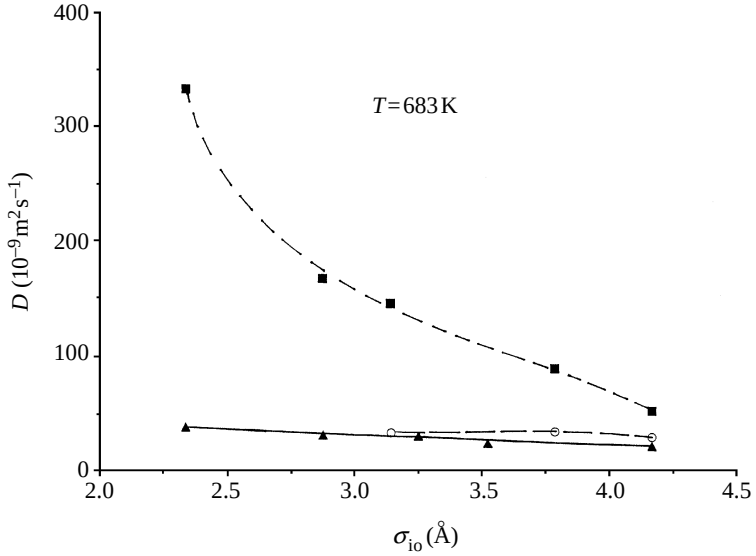

Figure 15. Diffusion coefficients of cations (▲), anions (○) and uncharged solutes or 'drones' (■) at 683 K and a solvent density of 0.35 g cm^{-3} as a function of the size represented by the Lennard–Jones parameter σ_{io} (from Noworyta *et al.* 2000).

at 298 K, and again weakly dependent on size. This implies that the structure of the hydrophilic solvation shells of small ions does not change much with temperature, but their dynamics depends strongly on the temperature. On the other hand, the hydration numbers of hydrophobic solutes and the residence times of the water of hydration depend strongly on temperature and solvent density.

The angularly averaged solute–water pair correlation functions in supercritical water are qualitatively different for ions and uncharged solutes, with water expelled from the region next to the uncharged solute, but compressed by the electric field in the neighbourhood of a small ion. This is reflected in the partial molar volumes $\bar{V}_2^\infty$ of ions and uncharged solutes, which are large and opposite in sign. $\bar{V}_2^\infty$ is positive for uncharged solutes and negative for ions and can be understood from the relation

$$\bar{V}_2^\infty = kT\kappa_T[1 - \rho_1 C_{12}^\infty], \tag{5.1}$$

which follows from the Kirkwood–Buff theory of solutions (Kirkwood & Buff 1952). Here, κ_T is the compressibility of the solvent, ρ_1 is the solvent density and C_{12}^∞ is the integral of the solute–solvent direct correlation function, which is related to the corresponding pair correlation function through the generalization of the Ornstein–Zernike equation for a two-component system. The compressibility κ_T is always positive and diverges at the critical point, which explains the large magnitude of the partial molar volumes in the supercritical region. The sign of the quantity in square brackets determines the sign of the partial molar volume. A useful approximation, for non-polar solutes, is to replace C_{12}^∞ by the second cross virial coefficient (Brelvi & O'Connell 1972; O'Connell 1981, 1994). This can be further approximated by the second virial coefficient of hard spheres, when the agreement of the calculated $\bar{V}_2$ with the simulations is quite good (Rasaiah *et al.* 2000).

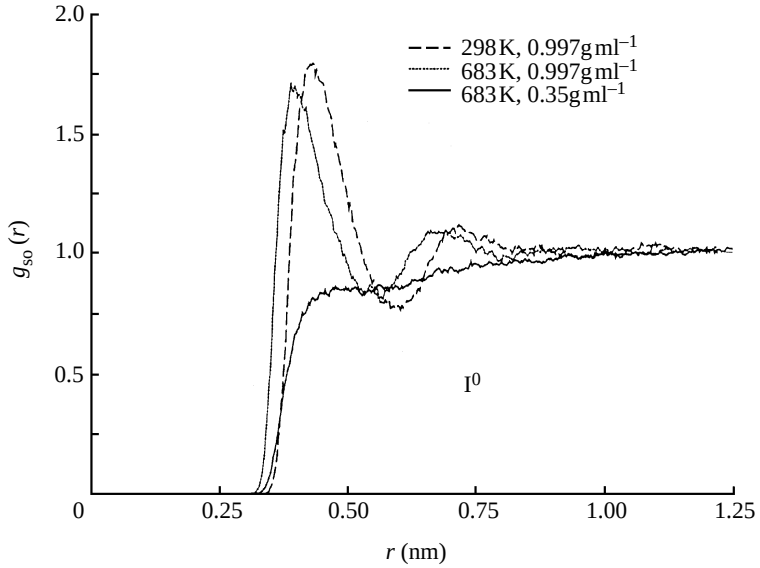

Figure 16. Solute–oxygen pair correlation functions for I^0 at 289 K and a solvent density of 0.997 g cm^{-3} compared with the corresponding results at 683 K at solvent densities of 0.35 g cm^{-3} and 0.997 g cm^{-3} (from Rasaiah *et al.* 2000).

The ion diffusion coefficients, determined by molecular dynamics simulation, are larger in magnitude at 683 K than at 298 K. They vary little with ion size at a solvent density of 0.35 g cm^{-3} and are nearly the same for cations and anions (Noworyta *et al.* 2000). This agrees with the experimental studies of Wood *et al.* (1995) and of Marshall and co-workers (Quist & Marshall 1968). Figure 15 shows the diffusion coefficients of ions and uncharged solutes at 683 K as a function of the size of anions (Noworyta *et al.* 2000), which should be compared with the corresponding diffusion coefficients at 298 K displayed in figure 6. The weak dependence on charge and size suggests that the mechanism of diffusion under supercritical conditions is quite different from what it is at room temperature.

In contrast to hydrophilic solvation, the hydrophobic hydration of a non-polar solute (or large ion) is sensitive to changes in both temperature and solvent density. This is strikingly clear in the solute–oxygen pair correlation for I^0 at 298 K and 683 K and at two different solvent densities (0.32 g cm^{-3} and 0.997 g cm^{-3}) displayed in figure 16.

The peak in the solute–solvent pair correlation function that is quite prominent at 298 K disappears at 683 K when the solvent density is close to the critical value of 0.32 g cm^{-3}, but is restored when the density is increased to 0.997 g cm^{-3}. This suggests a correlation with the solvent density rather than with the temperature. Furthermore, the characteristic behaviour of ions and uncharged solutes at room temperature (figure 6) that is absent at 683 K and a solvent density of 0.35 g cm^{-3} (figure 15) reappears when the solvent density is increased to 0.997 g cm^{-3}, as shown in a recent study (Noworyta *et al.* 2000). The diffusion coefficients of positive and negative ions lie on separate curves with distinct maxima when plotted as a function of size and small uncharged solutes diffuse faster than ions of the same size, while the opposite is true for large solutes. This implies that the dynamics of ions and neutral

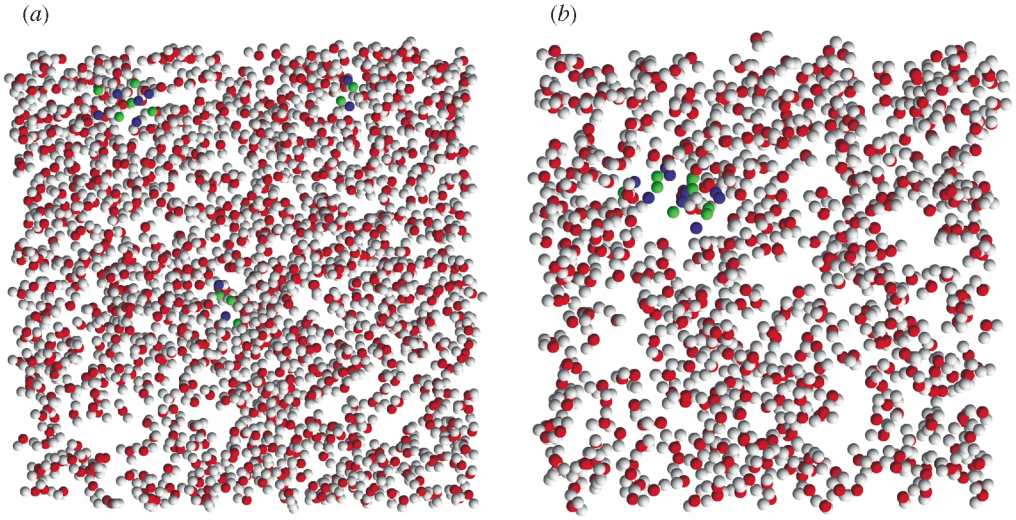

Figure 17. Snapshots of 0.5 molal and 1 molal NaCl aqueous solutions at 683 K. The oxygen and hydrogen atoms in water are represented as red and grey circles, respectively. Na^+ ions are represented in blue, and Cl^- ions in green. Note the presence of a single NaCl cluster in the 1 molal NaCl solution (*b*), whereas in the 0.5 molal NaCl solution there are three different NaCl clusters (*a*). The solvent density is 0.35 g cm^{-3} (from Koneshan & Rasaiah 2000).

solutes in aqueous solutions of supercritical water correlate with the solvent density as well as the temperature.

The dielectric constant of water is *ca.* 5 at 683 K and a density of 0.35 g cm^{-3}. Electrolytes are less soluble at high temperatures and multiple-ion association and cluster formation are predicted in supercritical aqueous electrolyte solutions (Brelvi & O'Connell 1972; O'Connell 1981, 1994). As noted earlier, the SPC/E model for water has critical parameters and dielectric constants close to those measured for real water. Computer simulations of aqueous sodium chloride solutions using the SPC (Cui & Harris 1995; Reagan *et al.* 1999) and SPC/E models confirm lower electrolyte solubility at elevated temperatures, and show that the individual diffusion coefficients and ion mobilities decrease with increasing electrolyte concentration (Koneshan *et al.* 2001; Koneshan & Rasaiah 2000; Rasaiah *et al.* 2000; Noworyta *et al.* 2000). They also confirm the presence of a distribution of clusters of positive and negative ions of varying size in which some ions are bridged by water molecules. There is an overall decrease in hydration numbers of the ions. Cluster formation between ions goes well beyond simple pairing of oppositely charged ions as predicted by Oelkers & Hegelson (1993). Sodium chloride solutions near saturation or super saturation (*ca.* 1 molal) at 683 K contain large clusters of positive and negative ions moving together, so that the diffusion coefficients of the individual ions Na^+ and Cl^- are nearly the same (Koneshan & Rasaiah 2000). Figure 17 shows equilibrium configurations of 0.5 M and 1.0 M sodium chloride in which the multiple and single clusters bridged by water molecules in these solutions are clearly visible.

The parameters of the SPC/E model were fitted to the equilibrium properties of water at 298 K. This might seem to be a serious drawback to our discussion of ionic solutions in the supercritical region in terms of this model. However, the

SPC/E model predicts the critical parameters and the dielectric constant of water in the supercritical region rather well. Improved models that incorporate the atomic polarizability of the oxygen and hydrogen atoms in water and ions have been proposed. Amongst these is the revised polarizability model (RPOL) developed by Dang (1992*b*), which is a modification of the SPC/E model. Smith & Dang (1994) studied the effect of this polarization on the potentials of mean force of sodium and chloride ions at room temperature and found it to be small but measurable. Koneshan *et al*. (2001) has shown that differences between the diffusion coefficients of ions calculated with the SPC/E and RPOL models are small at 298 K and also at 683 K. This means that calculations of the transport properties of ions at infinite dilution using the SPC/E at 683 K are not seriously compromised by the neglect of the temperature dependence of the induced polarizability in this model.

This study was supported by grant no. CHE 9961336 from the National Science Foundation and by grant GR/L08427 from the EPSRC. We thank our collaborators, S. Koneshan, S. H. Lee and J. P. Noworyta for their contributions to this research. J.C.R. thanks the Laboratory for Chemical Physics, NIDDK at the National Institutes of Health for their hospitality.

References

Allen, M. P. & Tildesley, D. J. 1987 *Computer simulation of liquids*. Oxford University Press.
Bagchi, B. 1989 *A. Rev. Phys. Chem.* **40**, 115.
Bagchi, B. & Biswas, R. 1998 *Acc. Chem. Res.* **31**, 18.
Bagchi, B. & Chandra, A. 1989 *J. Chem. Phys.* **90**, 7337.
Balbuena, P. B., Johnston, K. P. & Rossky, P. J. 1996 *J. Phys. Chem.* **100**, 2706.
Balbuena, P. B., Johnston, K. P., Rossky, P. J. & Hyun, J. K. 1998 *J. Phys. Chem.* B **102**, 3806.
Balucani, U. & Zoppi, M. 1994 *Dynamics of the liquid state*. Oxford University Press.
Berendsen, H. J. C., Grigera, J. R. & Straatsma, T. P. 1987 *J. Phys. Chem.* **91**, 6269.
Bergmann, D. L., Lyubartsev, A. P. & Laaksonen, A. 1999 *Phys. Rev.* E. **60**, 4482.
Berkowitz, M. & Wan, W. 1987 *J. Chem. Phys.* **86**, 376.
Biswas, R. & Bagchi, B. 1997*a* *J. Am. Chem. Soc.* **106**, 5946.
Biswas, R. & Bagchi, B. 1997*b* *J. Chem. Phys.* **106**, 5587.
Biswas, R., Roy, S. & Bagchi, B. 1995 *Phys. Rev. Lett.* **75**, 1098.
Born, M. 1920 *Z. Phys.* **1**, 221.
Boyd, R. H. 1961 *J. Chem. Phys.* **35**, 1281.
Brelvi, S. W. & O'Connell, J. P. 1972 *AIChE J.* **18**, 1239.
Calef, D. & Wolynes, P. G. 1983 *J. Chem. Phys.* **78**, 4145.
Chen, J. H. & Adelman, S. A. 1980 *J. Chem. Phys.* **72**, 2819.
Chong, C. & Hirata, F. 1998 *J. Chem. Phys.* **108**, 7339.
Chong, C. & Hirata, F. 1999*a* *J. Chem. Phys.* **110**, 1835.
Chong, C. & Hirata, F. 1999*b* *J. Chem. Phys.* **111**, 3654.
Colonomos, P. & Wolynes, P. G. 1979 *J. Chem. Phys.* **71**, 2644.
Cui, S. T. & Harris, J. G. 1995 *J. Phys. Chem.* **99**, 2900.
Dang, L. X. 1992*a* *Chem. Phys. Lett.* **200**, 21.
Dang, L. X. 1992*b* *J. Chem. Phys.* **97**, 2659.
Dang, L. X. 1995*a* *J. Am. Chem. Soc.* **117**, 6954.
Dang, L. X. 1995*b* *J. Chem. Phys.* **102**, 3483.
Dang, L. X. & Garrett, B. C. 1993 *J. Chem. Phys.* **99**, 2972,
Dang, L. X. & Kollmann, P. 1995 *J. Phys. Chem.* **99**, 55.

Eisenberg, H. & Kauzmann, W. 1969 *The structure and properties of water*. Oxford University Press.

Eley, D. D. 1939*a* *Trans. Faraday Soc.* **35**, 1281.

Eley, D. D. 1939*b* *Trans. Faraday Soc.* **35**, 1421.

Frank, H. S. 1966 In *Chemical physics of ionic solutions* (ed. B. E. Conway & R. G. Barradas), p. 60. Wiley.

Frank, H. S. & Evans, M. W. 1945 *J. Chem. Phys.* **13**, 507.

Franks, F. 1973 *Water, a comprehensive treatise*. New York: Plenum.

Frenkel, D. & Smit, B. 1996 *Understanding molecular simulation*. Academic.

Friedman, H. L., Ranieri, F. O., Peng, B.-C. & Newton, M. D. 1995 *J. Mol. Liq.* **65/66**, 7.

Fuoss, R. M. 1959 *Proc. Natl Acad. Sci. USA* **45**, 807.

Guillot, B. J. & Guissani, Y. 1993 *J. Chem. Phys.* **99**, 8075.

Guissani, Y. & Guillot, B. J. 1993 *J. Chem. Phys.* **98**, 8221.

Hornig, M. L., Gardecki, J., Papazyan, A. & Maroncelli, M. 1995 *J. Phys. Chem.* **99**, 17 311.

Hubbard, J. B. 1978 *J. Chem. Phys.* **68**, 1649.

Hubbard, J. B. & Kayser, R. F. 1981 *J. Chem. Phys.* **74**, 3535.

Hubbard, J. B. & Kayser, R. F. 1982 *J. Chem. Phys.* **76**, 3377.

Hubbard, J. B. & Onsager, L. 1977 *J. Chem. Phys.* **67**, 4850.

Hubbard, J. B. & Wolynes, P. 1985 Theories of solvated ion dynamics. In *The chemical physics of ion solvation* (ed. R. vR. Dogonadze, E. Kalman, A. A. Kornyshev & J. Ulstrup), part C, ch. 1. Elsevier.

Hubbard, J. B., Colonomos, P. &. Wolynes, P. G. 1979 *J. Chem. Phys.* **71**, 2652.

Impey, R. W., Madden, P. A. & MacDonald, I. R. 1983 *J. Phys. Chem.* **87**, 5071.

Jiminez, R., Fleming, G. R., Kumar, P. V. & Maroncelli, M. 1996 *Nature* **369**, 471.

Kirkwood, J. & Buff, R. P. 1952 *J. Chem. Phys.* **19**, 774.

Koneshan, S. & Rasaiah, J. C. 2000 *J. Chem. Phys.* **113**, 8125.

Koneshan, S., Lynden-Bell, R. M. & Rasaiah, J. C. 1998*a* *J. Am. Chem. Soc.* **120**, 12 041.

Koneshan, S., Rasaiah, J. C., Lynden-Bell, R. M. & Lee, S. H. 1998*b* *J. Phys. Chem.* **102**, 4193.

Koneshan, S., Rasaiah, J. C. & Dang, L. X. 2001 *J. Chem. Phys.* **114**, 7544.

Kubo, R., Toda, M. & Hashitsume, N. 1991 *Statistical physics*. II. *Non equilibrium statistical mechanics*, 2nd edn, p. 104. Springer.

Kumar, P. V. & Maroncelli, M. 2000 *J. Chem. Phys.* **112**, 5370.

Ladanyi, B. M. & Maroncelli, M. 1998 *J. Chem. Phys.* **109**, 3204.

Lynden-Bell, R. M. & Rasaiah, J. C. 1997 *J. Chem. Phys.* **107**, 1981.

Maroncelli, M. & Fleming, G. R. 1990 *J. Chem. Phys.* **92**, 3151.

Maroncelli, M., MacInnes, J. & Fleming, G. R. 1989 *Science* **243**, 1674.

Maroncelli, M., Kumar, P. V. & Papazyan, A. 1993 *J. Phys. Chem.* **97**, 13.

Neria, E. & Nitzan, A. 1992 *J. Chem. Phys.* **96**, 5433.

Nguyen, H. L. & Adelman, S. 1984 *J. Chem. Phys.* **81**, 4564.

Nichols III, L. & Calef, D. F. 1988 *J. Chem. Phys.* **89**, 3783.

Noworyta, J. P., Koneshan, S. & Rasaiah, J. C. 2000 *J. Am. Chem. Soc.* **122**, 11 194.

O'Connell, J. P. 1981 *Fluid Phase Equilib.* **6**, 21.

O'Connell, J. P. 1994 Thermodynamics and fluctuation solution theory with some applications to systems at or near supercritical conditions. In *Supercritical fluids fundamentals and applications* (ed. E. Kiran & J. M. H. Levelt Sengers). NATO ASI series, vol. 271. Kluwer.

Oelkers, E. H. & Hegelson, H. G. 1993 *Science* **261**, 888.

Perera, L. & Berkowitz, M. 1992 *J. Chem. Phys.* **97**, 5253.

Quist, A. S. & Marshall, W. L. 1968 *J. Phys. Chem.* **72**, 684.

Raineri, F. O. & Friedman, H. L. 1994 *J. Chem. Phys.* **101**, 6111.

Raineri, F. O., Resat, H., Peng, B.-C., Hirata, F. & Friedman, H. L. 1994 *J. Chem. Phys.* **100**, 1477.

Raineri, F. O., Zhou, Y., Friedman, H. L. & Stell, G. 1991 *Chem. Phys.* **152**, 201.

Raineri, F. O., Friedman, H. L., Perng, B.-C. & Brandariz, I. 1996 Molecular theory of solvation dynamics, with applications to ultrafast spectroscopy. In *Femtochemistry: ultrafast chemical and physical processes in molecular systems* (ed. M. Chergui). World Scientific.

Rasaiah, J. C., Noworyta, J. P. & Koneshan, S. 2000 *J. Am. Chem. Soc.* **122**, 11 182.

Re, M. & Laria, D. 1997 *J. Phys. Chem.* **101**, 10 494.

Reagan, M. T., Harris, J. G. & Tester, J. W. 1999 *J. Phys. Chem.* B **103**, 7936.

Rips, I. 1994 *AIP Conf. Proc. Ser.* **298**, 334.

Rips, I., Klafter, J. & Jortner, J. 1988*a* *J. Chem. Phys.* **88**, 3246.

Rips, I., Klafter, J. & Jortner, J. 1988*b* *J. Chem. Phys.* **89**, 4288.

Robinson, R. A. & Stokes, R. H. 1959 *Electrolyte solutions*, 2nd edn. Butterworths.

Rosenthal, S., Jiminez, R., Fleming, G. R., Kumar, P. V. & Maroncelli, M. 1994 *J. Mol. Liq.* **60**, 25.

Sirdhar, G., Vijaykumar, P. & Tembe, B. L. 1993 *J. Chem. Phys.* **99**, 43 147.

Sivaprasad, K. R., Prasad, V., Manjula Devi, K. & Tembe, B. L. 1994 *Proc. Ind. Acad. Sci.* **106**, 467.

Smith, D. E. & Dang, L. X. 1994 *J. Chem. Phys.* **100**, 3757.

Soper, A. K., Bruni, F. & Ricci, M. A. 1997 *J. Chem. Phys.* **106**, 24 712.

Stillinger, F. 1980 *Science* **209**, 451.

Tester, J. W., Marrone, P. A., DiPhillipo, M. M., Sako, K., Reagan, M. T., Arias, T. & Peters, W. 1998 *J. Supercrit. Fluids* **13**, 225.

Tucker, S. C. 1999 *Chem. Rev.* **99**, 391.

Vijaykumar, P. & Tembe, B. L. 1991 *J. Phys. Chem.* **95**, 6430.

Walker, G. C., Akesson, E., Johnson, A. E., Levinger, N. E. & Barbara, P. F. 1992 *J. Phys. Chem.* **96**, 3728.

Wilson, M. A., Pohorille, A. & Pratt, L. R. 1985 *J. Chem. Phys.* **83**, 5832.

Wolynes, P. G. 1978 *J. Chem. Phys.* **68**, 473.

Wolynes, P. G. 1980 *A. Rev. Phys. Chem.* **31**, 345.

Wolynes, P. G. 1987 *J. Chem. Phys.* **86**, 5133.

Wood, R. H., Gruszkiewicz, M. S. & Zimmerman, G. H. 1995 *J. Phys. Chem.* **99**, 11 612.

Zwanzig, R. 1963 *J. Chem. Phys.* **38**, 1603.

Zwanzig, R. 1970 *J. Chem. Phys.* **52**, 3625.